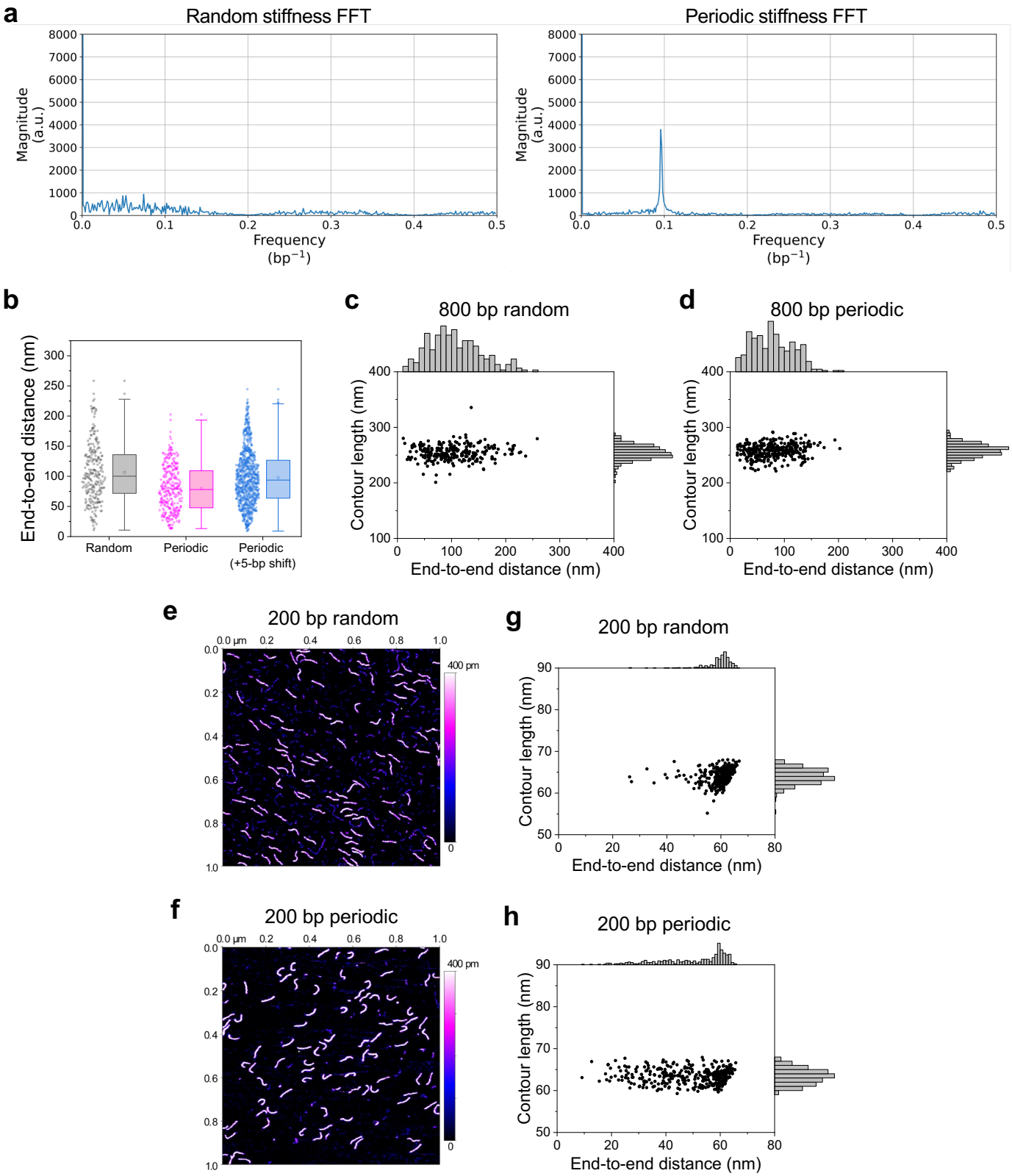

Extended Data Figure 1. AFM analysis of DNAs with periodic stiffness. a, Fast Fourier transform profiles of 800-bp DNAs with random or periodic stiffness. **b,** End-to-end distances of 800 bp DNAs with random, periodic, and phase-shifted periodic stiffness. **c-d,** Scatter plots of contour length versus end-to-end distance for 800-bp DNAs with random (**c**) and periodic (**d**) stiffness. **e-f,** Representative AFM images of 200-bp DNAs with random (**e**) and periodic (**f**) stiffness. **g-h,** Scatter plots of contour length versus end-to-end distance for 200-bp DNAs with random (**g**) and periodic (**h**) stiffness.

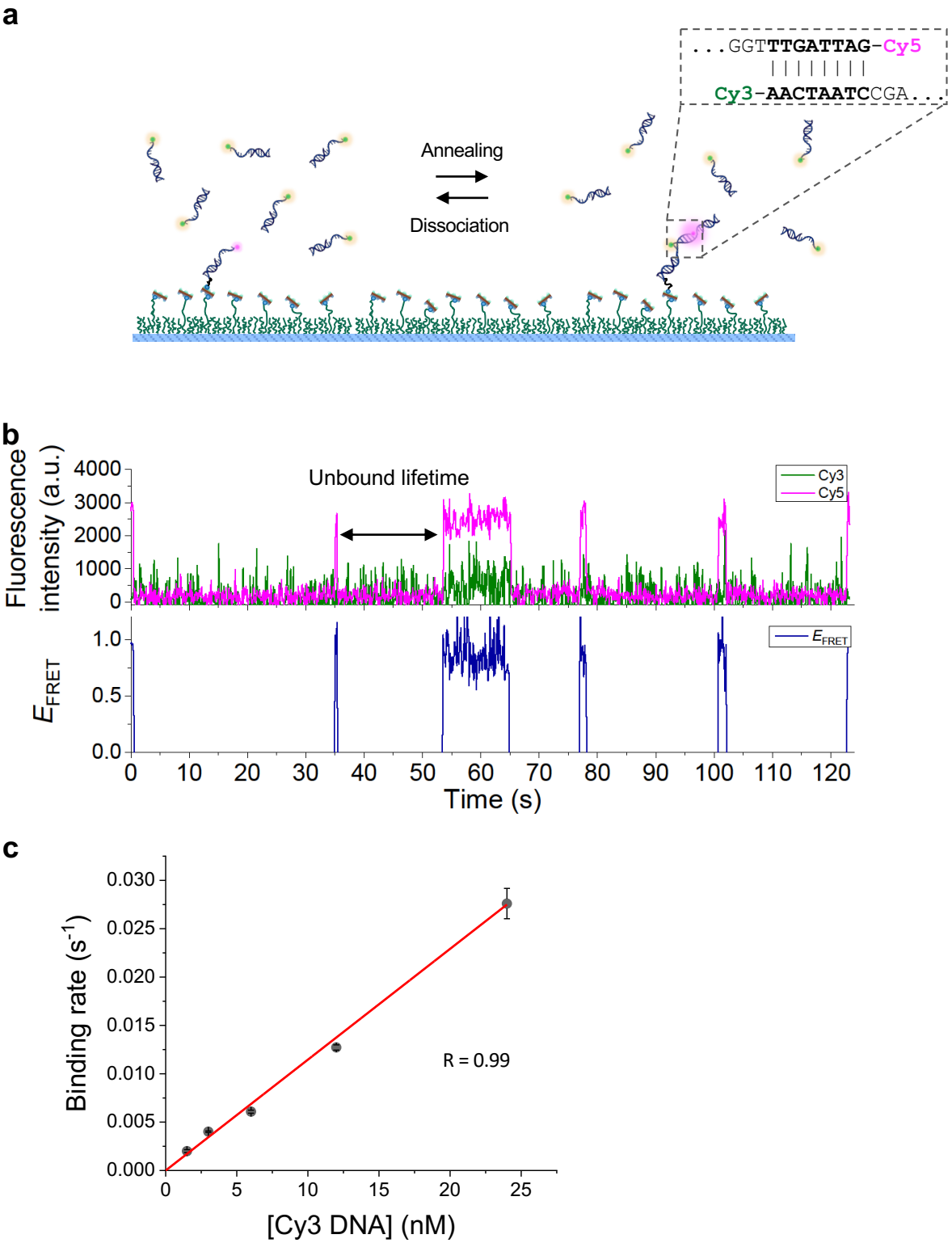

Extended Data Figure 2. Characterization of binding kinetics between sticky ends. a, Schematic of smFRET measurement of the association rate between two partially single-stranded DNA molecules sharing an 8-bp homology with 3-base gaps, as used in the looping rate measurements. **b,** Representative time traces of Cy3 and Cy5 fluorescence intensities and E_{FRET}. The binding rate was calculated as the inverse of the mean unbound lifetime. **c,** Binding rate measured at varying concentrations of the Cy3-labeled DNA and fitted to a straight line starting at the origin. The association rate constant (k_{on}) between the sticky ends was determined as the slope of the fit.

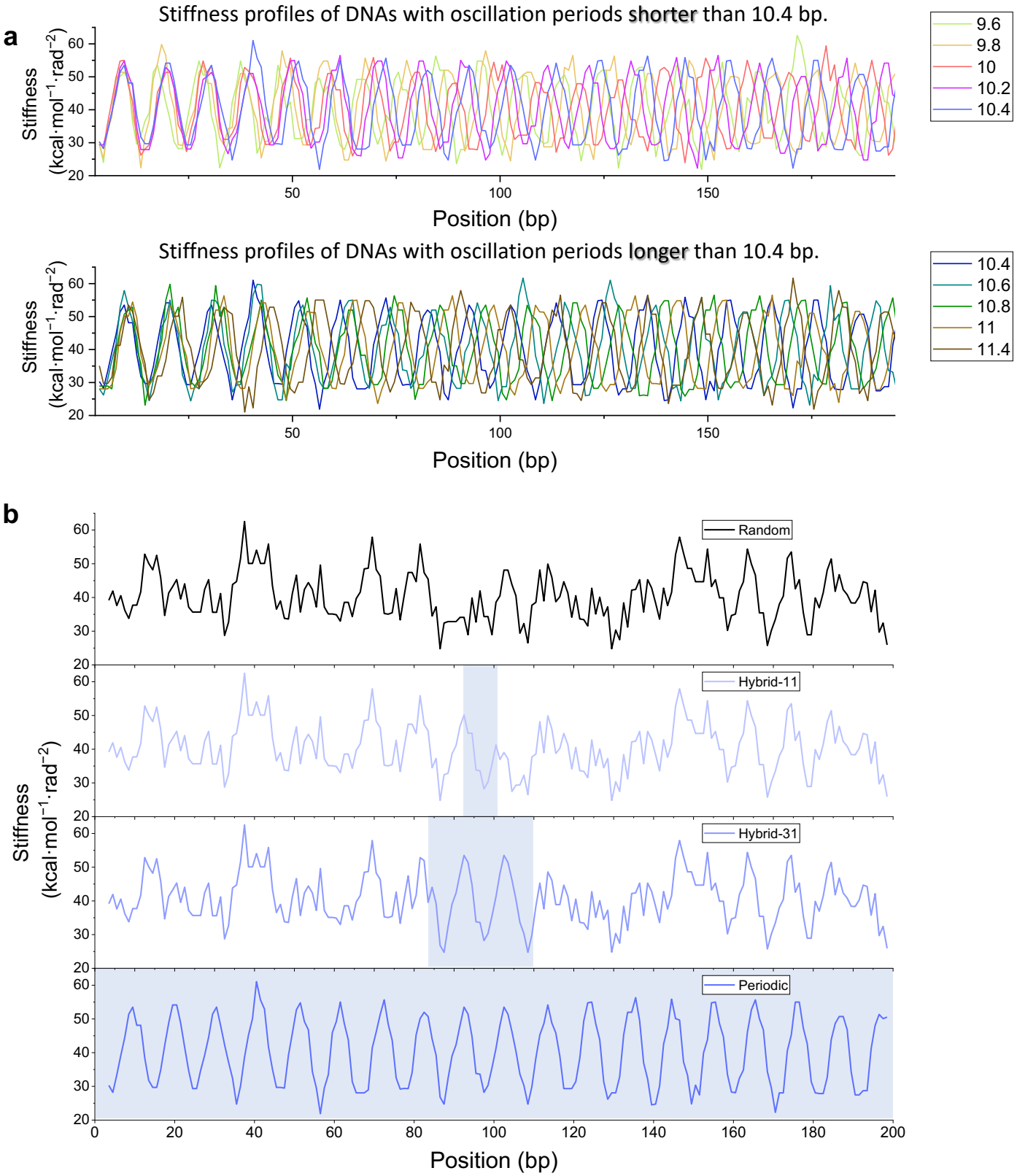

Extended Data Figure 3. Stiffness profiles of 200 bp DNAs. a, Stiffness profiles of 200 bp DNAs (5-bp moving average), grouped based on oscillation periods shorter or longer than 10.4 bp. **b,** Stiffness profiles of 200 bp DNAs containing partial periodic regions (11 bp or 31 bp) in the central region, compared with those of 200 bp DNAs with fully random or periodic stiffness.

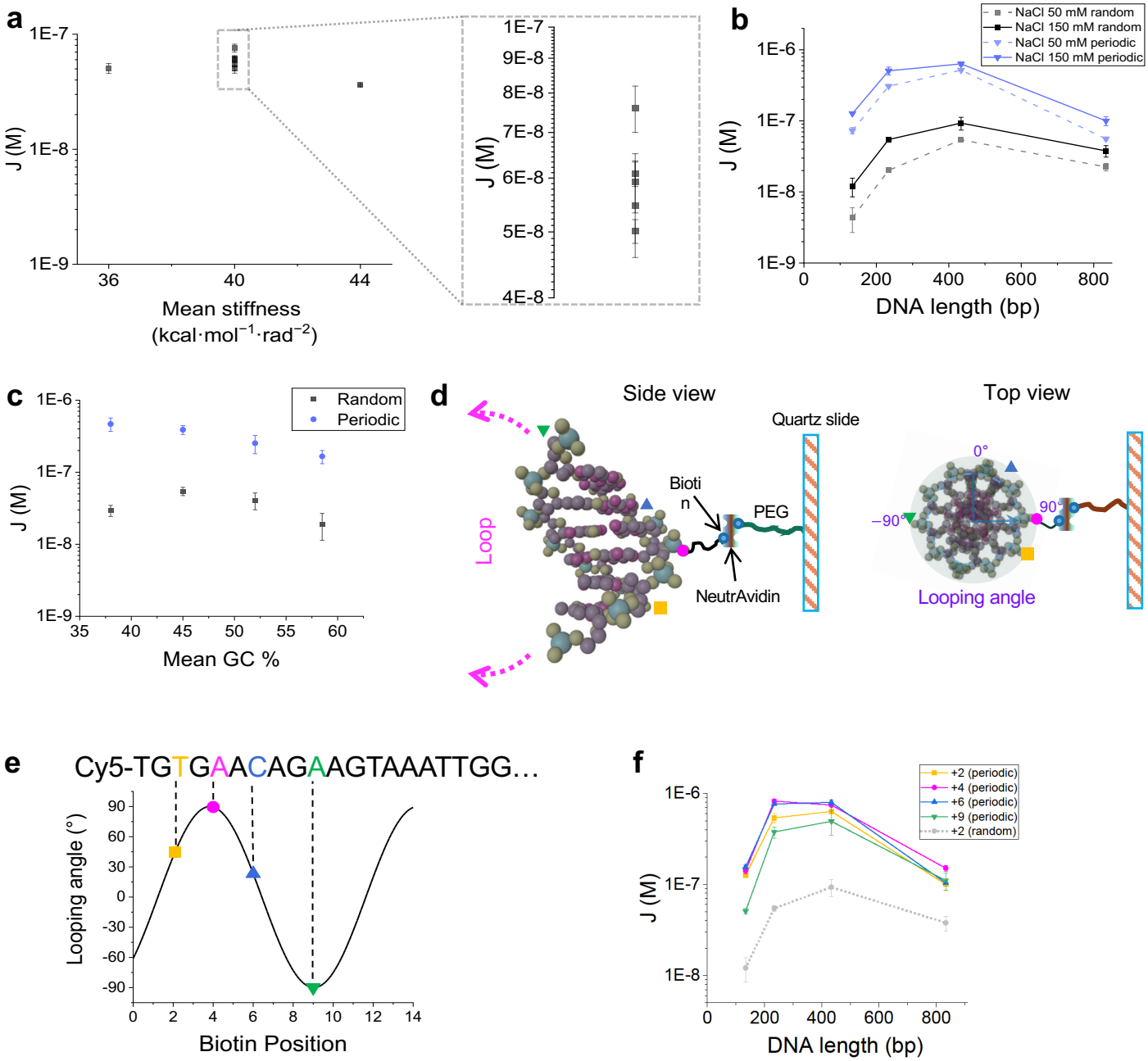

Extended Data Figure 4. Dependence of DNA looping rate on mean stiffness, salt concentration, GC content, and biotin position. a, J factors of 200-bp DNAs with varying mean stiffness. The inset shows data from five different DNA constructs with a mean stiffness of 40 kcal·mol^{-1}·rad^{-2}. All other sequence designs have a mean stiffness close to 40 kcal·mol^{-1}·rad^{-2}. **b,** J factors of DNAs with random and periodic stiffness measured at 50 mM and 150 mM NaCl. All other data were measured at 150 mM NaCl. **c,** J factors of 200-bp DNAs with random and periodic stiffness at varying GC contents. **d,** Schematic side and top views of a DNA molecule illustrating different biotin positions for surface tethering. The looping angle is defined as the angle between the preferred looping orientation (magenta arrows) and the surface (–90°: looping away from the surface; +90°: looping toward the surface). **e,** Looping angle as a function of biotin position. The preferred looping orientation was determined from the phase of the stiffness oscillation. **f,** J factors of periodic-stiffness DNAs of varying length measured for different biotin positions. J factors of random-stiffness DNAs are shown for comparison (gray, dotted line).

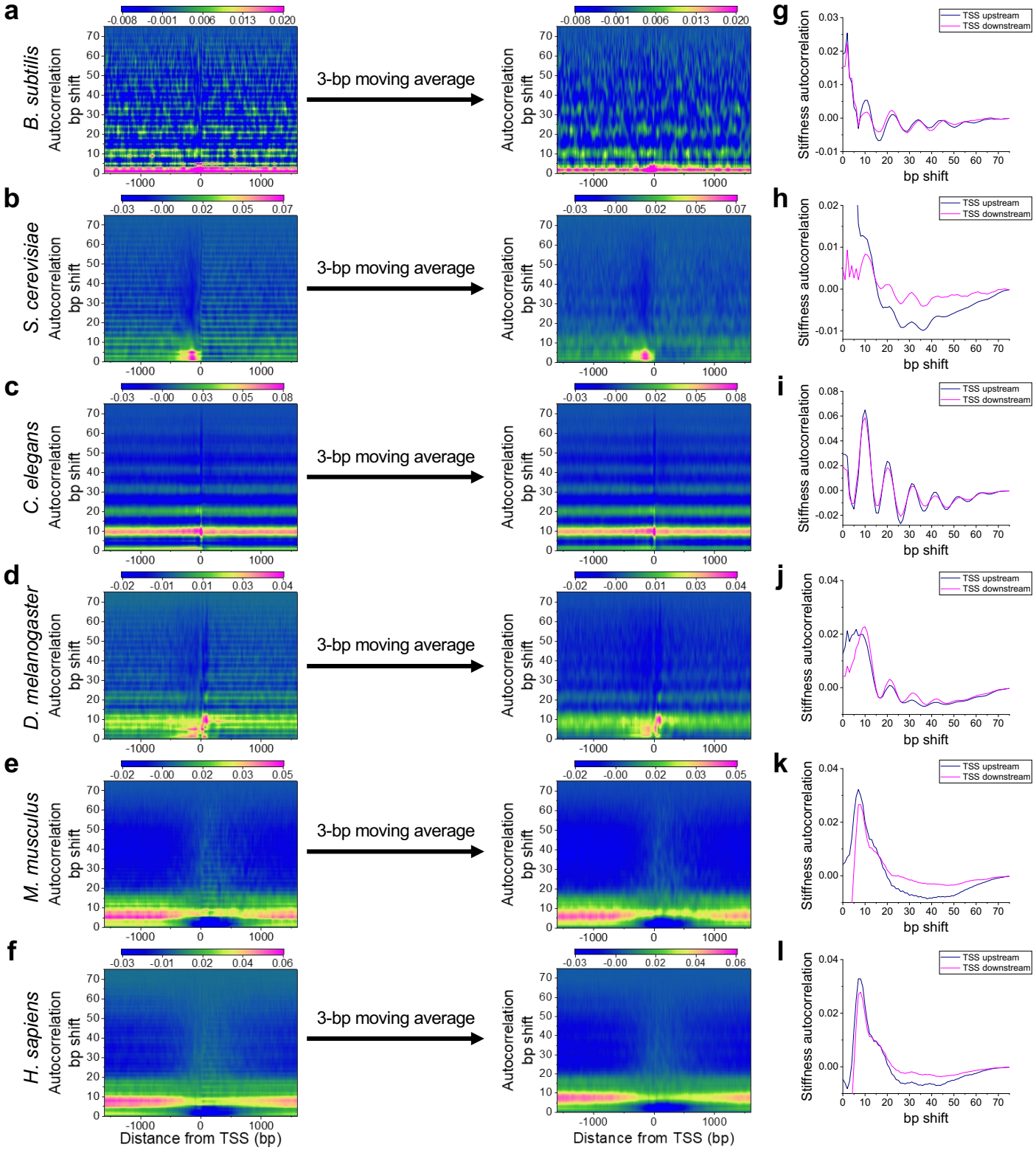

Extended Data Figure 5. Stiffness autocorrelation spectrograms near TSS across species. a-f, Gene-averaged stiffness autocorrelation spectrograms near TSS for *B. subtilis* (**a**), *S. cerevisiae* (**b**), *C. elegans* (**c**), *D. melanogaster* (**d**), *M. musculus* (**e**), and *H. sapiens* (**f**). The right panels show the spectrograms after applying a 3-bp moving average to remove periodicity arising from codon usage bias. **g-l,** Stiffness autocorrelation profiles computed for regions upstream (−500 to 0 bp) and downstream (0 to +500 bp) relative to the TSS.

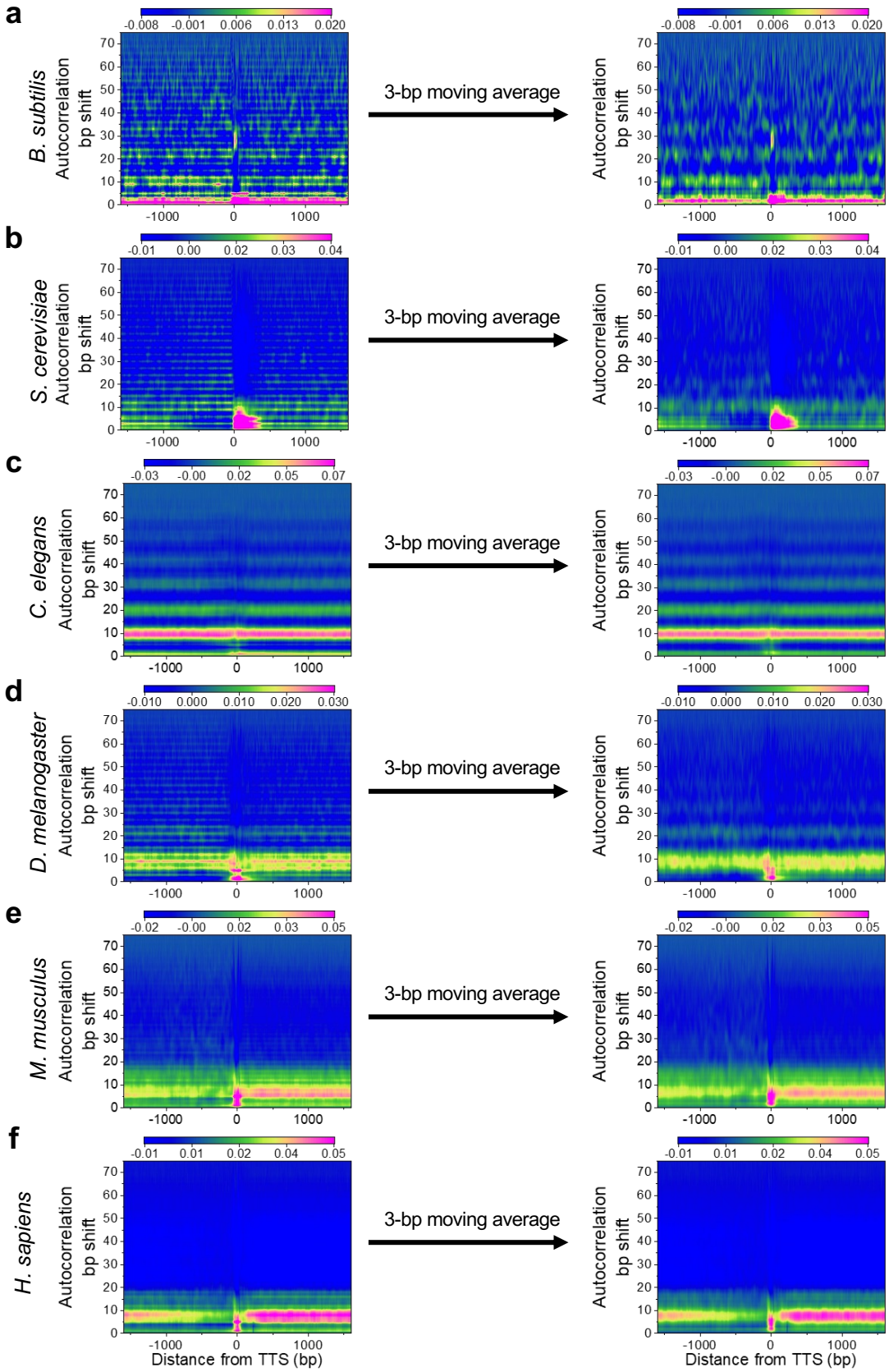

Extended Data Figure 6. Stiffness autocorrelation spectrograms near transcription termination sites (TTS) across species. a-f, The same analysis as in Extended Data Fig. 5 was applied to genomic regions near TTS for each species. Similar patterns of 10.4-bp stiffness periodicity were observed, overlaid with 3-bp stiffness periodicity and accompanied by characteristic perturbations at the TTS.

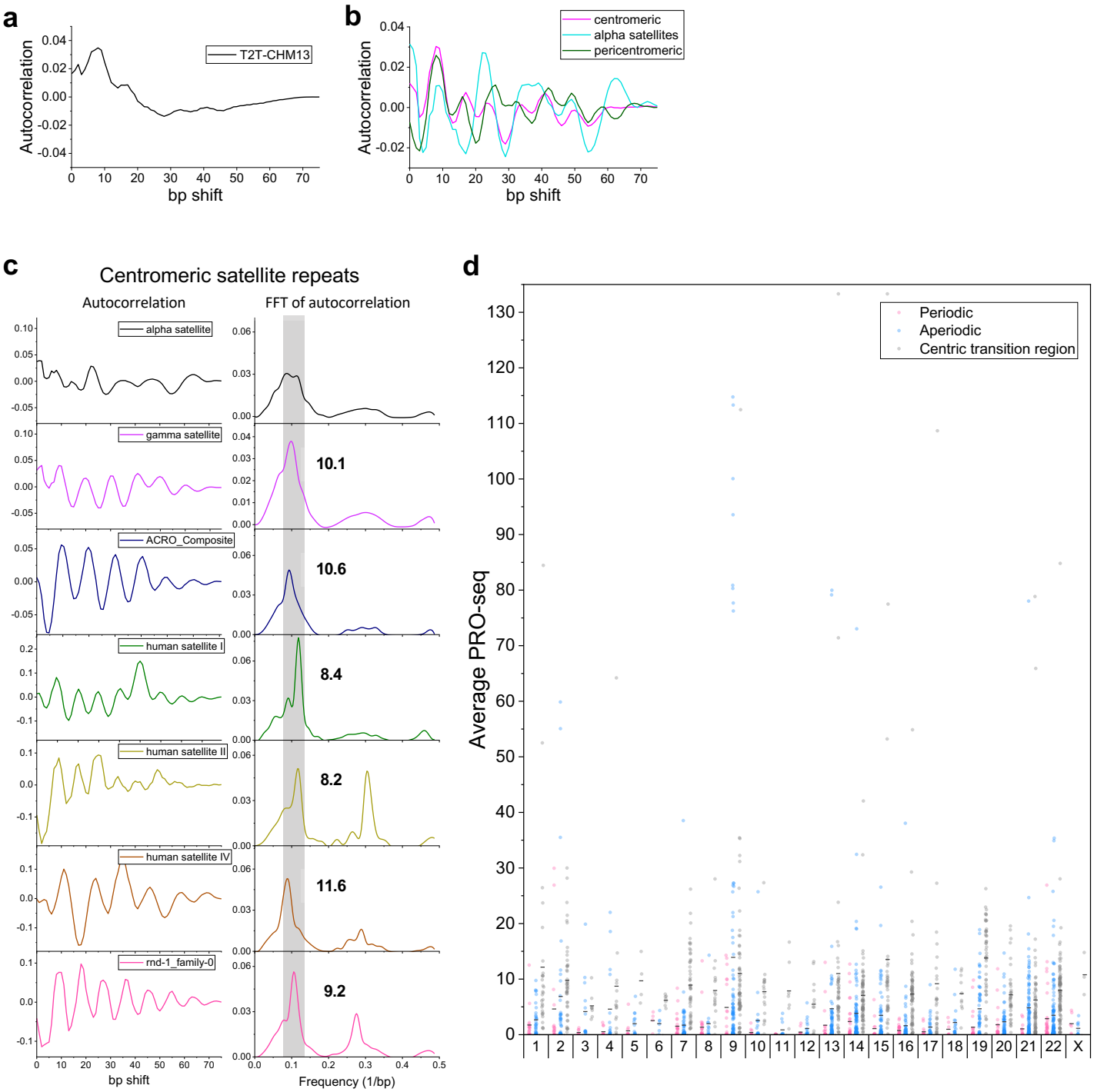

Extended Data Figure 7. Diversity of stiffness periodicity in human centromeres and the correlation between periodicity and transcriptional activity. a, Stiffness autocorrelation profile of the entire T2T-CHM13 genome. **b,** Stiffness autocorrelation profiles of centromeric regions (magenta), alpha satellites (teal), and pericentromeric regions (black). **c,** Stiffness autocorrelation profiles of different centromeric satellite families (left) and their corresponding fast Fourier transform (FFT) spectra (right). Low-frequency background was removed from the FFT spectra to reveal the peaks representing oscillations (Materials and Methods). The resulting spectra show marked differences in the positions of the primary frequency peaks (gray shaded regions, bold labels). **d,** Distributions of transcriptional activity for periodic (magenta) and aperiodic (cyan) centromeric regions, as well as centric transition regions (gray), are compared across chromosomes. Average PRO-seq signals were calculated as the mean of PRO-seq signals from each annotated satellite region (Table S3).

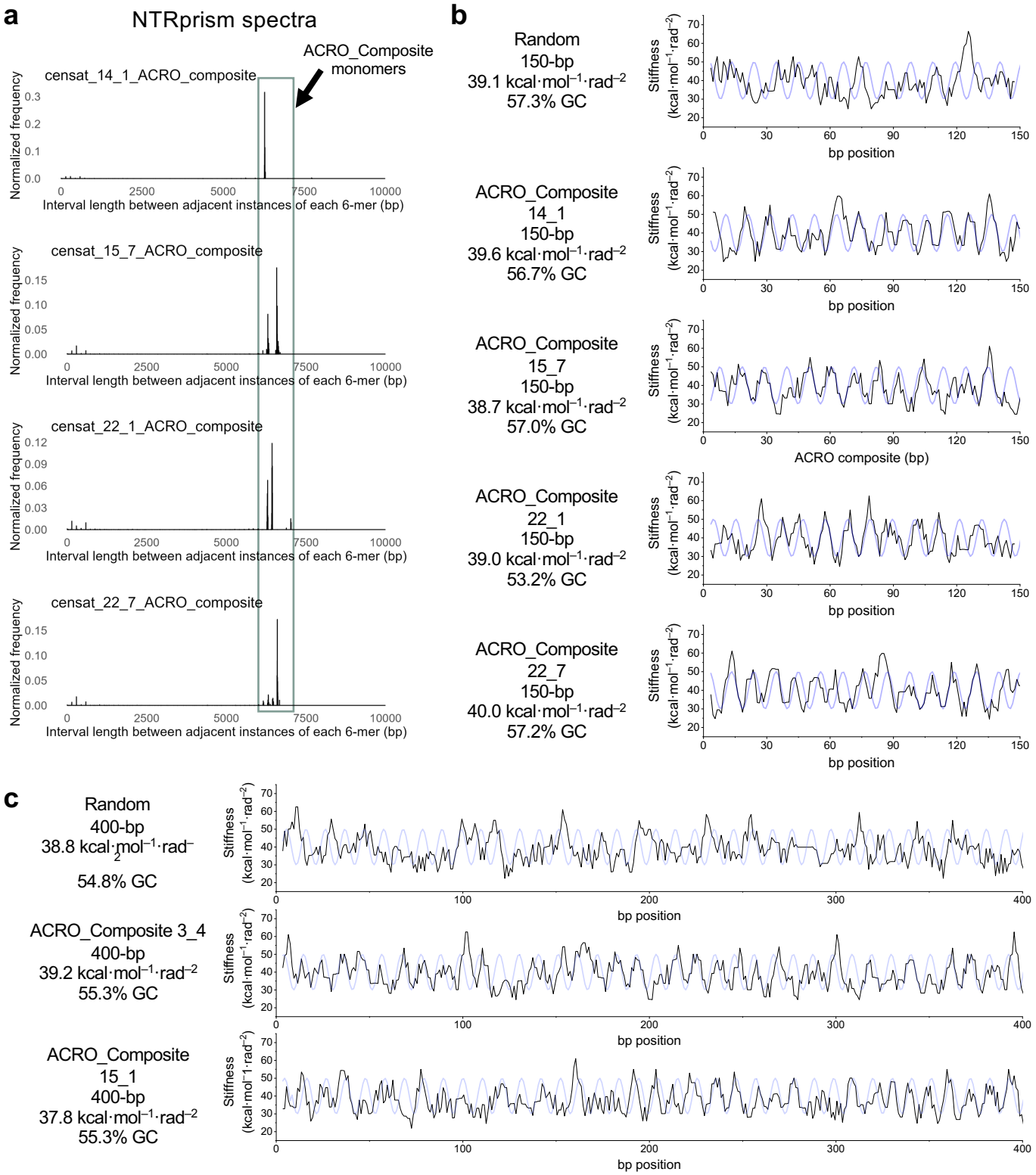

Extended Data Figure 8. Design of ACRO_Composite repeat sequences for single-molecule measurements. **a,** NTRprism spectra for various ACRO_Composite subfamilies in chromosomes 3, 14, 15, and 22. The spacing between monomer sizes indicates a minimal repeating unit of ~150 bp. **b,** Stiffness profiles of 150-bp ACRO_Composite sequences selected from different genomic regions for smFRET measurements, compared with a 150-bp random-stiffness sequence. A sinusoidal curve with a 10.6-bp period is shown as a reference (blue lines). Mean stiffness and GC content are indicated. **c,** Stiffness profiles of 400-bp ACRO_Composite sequences selected from chromosomes 3 and 15 for AFM measurements, compared with a 400-bp random-stiffness sequence. A sinusoidal curve with a 10.6-bp period is shown as a reference (blue lines). Mean stiffness and GC content are indicated.